Review Article

Molecular dynamics simulations of metal-electrolyte interfaces under potential control

Linnéa Andersson and Chao Zhang

Abstract
The interfaces between metal electrodes and liquid electrolytes are prototypical in electrochemistry. That is why it is crucial to have a molecular and dynamical understating of such interfaces for both electrical properties and chemical reactivities under potential control. In this short review, we will categorize different schemes for modeling electrified metal-electrolyte interfaces used in molecular dynamics simulations. Our focus is on the similarities between seemingly different methods and their conceptual connections in terms of relevant electrochemical quantities. Therefore, it can be used as a guideline for developing new methods and building modularized computational protocols for simulating electrified interfaces.

Addresses
Department of Chemistry-Ångström Laboratory, Uppsala University, Lägerhyddsvägen 1, BOX 538, Uppsala, 75121, Sweden

Corresponding author: Zhang, Chao (chao.zhang@kemi.uu.se)
🐦🐦 (Zhang C.)

Introduction

The metal-electrolyte interface plays a key role in electrochemical energy storage and conversion. In general, there are two kinds of *idealized* electrodes: ideal polarizable and ideal non-polarizable. The former as exemplified by the Hg electrode involves only capacitive charging and zero exchange current (density); the latter, taking the example of the Ag/AgCl electrode, allows free passing of Faradic current with zero charge transfer resistance [1]. Different from the meaning of dipole-moment density in physical chemistry, polarization here refers to the applied potential. In other words, an ideal polarizable electrode can sustain an applied potential and form an electric double layer. Therefore, a realistic computational model of the metal-electrolyte interface under electrochemical conditions should include the effects of an external potential.

Despite that the grand canonical (GC) formulation of density functional theory (DFT) was introduced right after the birth of canonical DFT in the mid-60s [2], its implementation for a slab system which resembles a metal-electrolyte interface in electronic structure calculation came out much later. Notably, Lovozoi et al. [3] discussed the strategies of applying GC-DFT to metal slab systems under periodic boundary conditions (PBCs) already in 2001. In particular, they realized that PBCs convoluted the electrostatic potential of systems *with a net charge* because of the homogeneous compensating background and that an electrostatic correction must be applied to restore the physical one.

Parallel to the development of GC-DFT approaches, attempts were made to use charge transfer from ions to the metal interface to mimic the electrified interfaces with canonical DFT. Early examples were given by Skúlason et al. [4] and Rossmeisl et al. [5] around 2007, where different numbers of hydrogen atoms were added at the Pt-water interface, to study the system at different electrode potentials. In these setups, the hydrogen atoms turn to solvated protons in the water bilayer and release electrons to the metal surface, which provides a static model of the electric double layer.

Since metal-electrode interfaces involve both electronic and ionic responses (to an external potential), a dynamical picture of such interfaces beyond a static DFT description is clearly needed. The pioneering work in this direction was done by Price and Halley in 1995 [6]. They carried out the first Car-Parrinello-type molecular dynamics (MD) simulations of metal-water slab systems with an applied potential difference between the slabs (of 1.36 V), plane-wave basis set, and local pseudopotential.

These seminal works that developed independently have influenced later theoretical works that try to describe structural, dynamical, and electronic properties of electrified interfaces between metal electrode and

electrolyte solution on an equal footing. Therefore, an up-to-date view of this topic is desirable. On this note, we will focus on works based on DFTMD approaches and highlight the recent method developed in this field. Thus, discussions on their applications in electrocatalysis and electrochemical energy storage can be found in excellent reviews elsewhere [7–13]. Furthermore, we will only include methods based on equilibrium calculations; therefore, non-equilibrium methods such as Green's functions [14] are not discussed here.

In the following, we will first introduce necessary concepts in electrochemistry, which will help us to understand the motivation and the strategies behind different types of methods. Then, we will sort seemingly different methods into three categories and discuss examples in each type of method. Finally, a summary and outlook for future developments is also given.

Theoretical background
Fermi level and electrode potential

The work function of a metal surface W_e^{M} is defined as the energy required to take an electron from it into vacuum. For bulk metal, it is well-known that the opposite of the metal work function equals to the Fermi level of the metal $E_{\mathrm{F}}^{\mathrm{M}}$. The Fermi level is equal to the electrochemical potential $\tilde{\mu}_e^{\mathrm{M}}$, which can be partitioned into the chemical potential μ_e^{M} and the contribution from the Galvani potential ϕ^{M} (see Figure 1a for illustration):

$$E_{\mathrm{F}}^{\mathrm{M}} = \tilde{\mu}_e^{\mathrm{M}} = \mu_e^{\mathrm{M}} - \phi^{\mathrm{M}} e_0 = -W_e^{\mathrm{M}} \tag{1}$$

Then, the corresponding thermodynamic electrode potential will be written as:

$$U^{\mathrm{M}} = W_e^{\mathrm{M}} / e_0 \tag{2}$$

where the electron charge is defined as $-e_0$.

Similarly, the thermodynamic electrode potential of metal in solution equals to the work function of metal in solution (see Figure 1b).

$$U_{\sigma=0}^{\mathrm{M|S}}(\mathrm{abs}) = W_e^{\mathrm{M|S}} / e_0 \tag{3}$$

This is a key conclusion from a series of works from Trasatti and elaborated in Section 2.4 in the study by Cheng et al. [15]. In the expression above, we emphasize that the work function is well-defined when the surface charge σ is zero as by definition it does not include any contributions from the Volta potential ψ (see Figure 1a and its caption). Subsequently, it means the corresponding Fermi level of the metal electrode in solution can be expressed as:

$$E_{\mathrm{F},\sigma=0}^{\mathrm{M|S}} = -W_e^{\mathrm{M|S}} \tag{4}$$

For the electrified metal-electrolyte interface, the double-layer potential ϕ_{EDL} will be built up and this leads to the expression of the Fermi level as:

$$E_{\mathrm{F}}^{\mathrm{M|\,S}} = E_{\mathrm{F},\sigma=0}^{\mathrm{M|S}} - e_0 \phi_{\mathrm{EDL}} \tag{5}$$

In addition, by definition, the double-layer potential is also equal to the change in the Galvani potential difference $_{\mathrm{S}}\Delta_{\mathrm{M}}\phi = \phi^{\mathrm{M}} - \phi^{\mathrm{S}}$ between metal (M) and solution (S), i.e.

$$\phi_{\mathrm{EDL}} = {}_{\mathrm{S}}\Delta_{\mathrm{M}}\phi - {}_{\mathrm{S}}\Delta_{\mathrm{M}}\phi^{\sigma=0} \tag{6}$$

As noted by Trasatti, despite "that the experimentally measured potential has nothing to do with the actual electric potential drop across the interface" [16], they change by the same amount when the metal electrode is polarized. Thus, one can adjust the change in the Fermi level of metal-electrolyte interfaces in order to control the double-layer potential.

$$\Delta E_{\mathrm{F}}^{\mathrm{M|S}} = -e_0 \Delta({}_{\mathrm{S}}\Delta_{\mathrm{M}}\phi) = -e_0 \phi_{\mathrm{EDL}} \tag{7}$$

As shown in Section 3, this idea is exploited in GC-DFT or constant Fermi DFTMD, in which the total number of electrons in the system is varied in order to control the *change* in the Fermi level.

Charge transfer and volta potential

The alternative way to realize the "constant potential" is through charge transfer within the whole system itself (in contrast to the external reservoir). In the following, we will use two examples to illustrate this point.

Supposing that we have two metal species α and β. When they are separated apart, the electrochemical potential or the Fermi level of each species is:

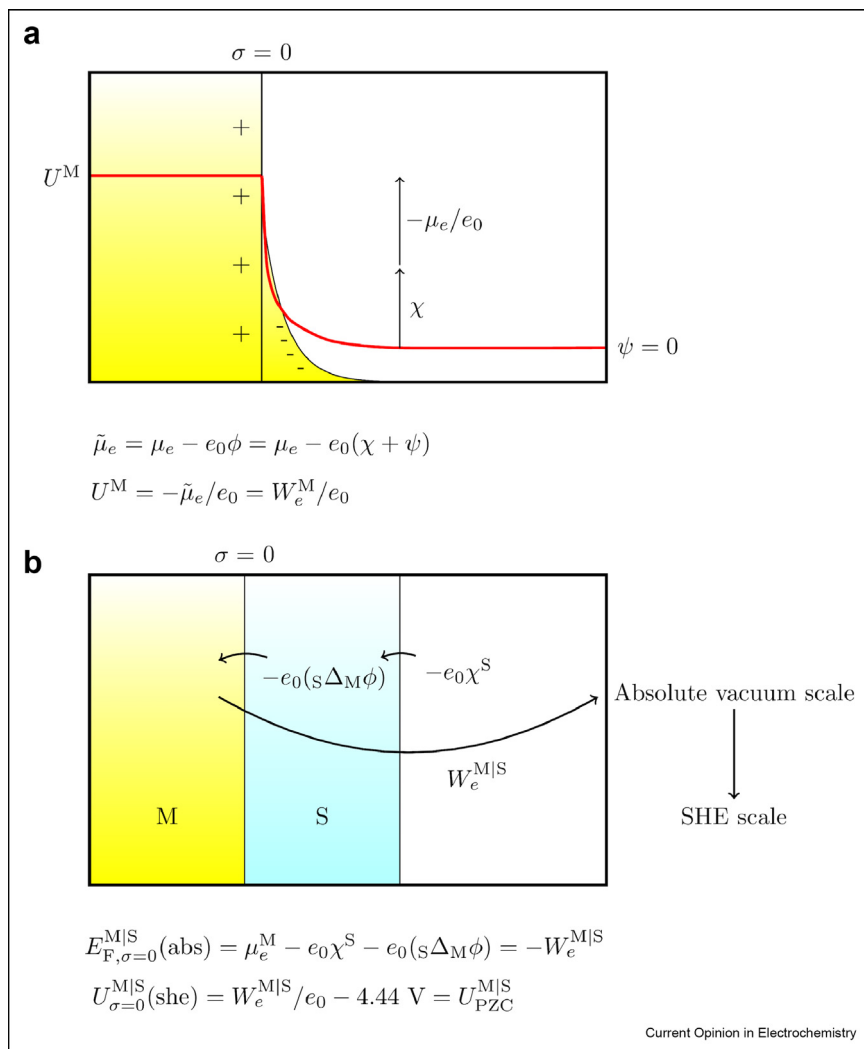$$\tilde{\mu}_e^{\alpha} = \mu_e^{\alpha} - e_0 \chi^{\alpha} \tag{8}$$

$$\tilde{\mu}_e^{\beta} = \mu_e^{\beta} - e_0 \chi^{\beta} \tag{9}$$

where μ is the chemical potential and χ is the surface potential (see Figure 1a and its caption).

Then, we put them in contact, as shown in Figure 2a. Supposing $\tilde{\mu}_{\beta}$ is more negative than $\tilde{\mu}_{\alpha}$, then a charge transfer will take place and the two metal species will become electrified. Now, the electrochemical potential of each species is:

$$\tilde{\mu}_e^{\prime\alpha} = \mu_e^{\alpha} - e_0 \chi^{\alpha} - e_0 \psi^{\alpha} \tag{10}$$

Figure 1

Metal interfaces with vacuum and solution. (**a**) Metal-vacuum interface. The electrochemical potential $\widetilde{\mu}_e$ consists of the chemical potential $\widetilde{\mu}$ and a contribution from the Galvani potential ϕ. The Galvani potential is composed of the Volta potential ψ due to net surface charge and the surface (dipole) potential χ. With zero surface charge, $\psi = 0$. (**b**) Metal-solution-vacuum interfaces. The work function $W_e^{M|S}$ is defined as the energy required to take an electron from the metal through the solution and into vacuum. The potential of zero charge $U_{pzc}^{M|S}$ can be calculated from this work function if the reference is changed from vacuum to standard hydrogen electrode (SHE).

$$\widetilde{\mu}_e'^{\beta} = \mu_e^{\beta} - e_0\chi^{\beta} - e_0\psi^{\beta} \tag{11}$$

where the Volta potential ψ is no longer zero.

The electrochemical potential of two metal species in contact must be the same. This means the chemical potential, the surface potential, and the Volta potential have the following relation:

$$e_0(_{\beta}\Delta_{\alpha}\psi) = e_0(\psi^{\alpha} - \psi^{\beta}) \tag{12}$$

$$= \mu_e^{\alpha} - e_0\chi^{\alpha} - (\mu^{\beta} - e_0\chi^{\beta}) \tag{13}$$

$$= W_e^{\beta} - W_e^{\alpha} \tag{14}$$

where we have used the relation between the work function, the chemical potential, and the surface potential. It is worth noting that in this conceptualization, the change in the surface potential χ upon contact is not considered.

The significance of the above equations is that the system of two metal species in contact is actually under a constant potential since the work function of each
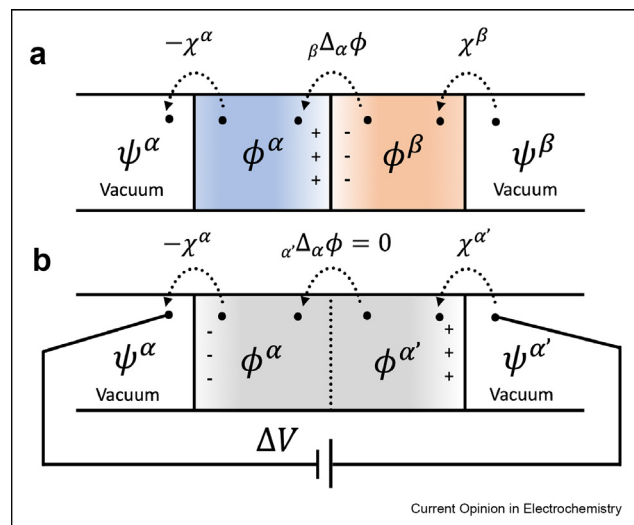
Generating the Volta potential difference due to charge transfer. (**a**) Two metals of different species in contact in which the metal α has a smaller work function. The Volta potential difference equals to the opposite of the work function difference. (**b**) Two metals of the same species in contact under an applied voltage ΔV. The Volta potential difference equals to the applied voltage. The definition of symbols can be found in the Text.

metal species is an intrinsic material's property. This means one could use a counter-electrode or counter-ion which has a different work function to control the Volta potential difference.

Along the same line, the follow-up example is two metals of the same species in contact under an external voltage ΔV (Figure 2b). Since two metals must be in equilibrium, this implies:

$$e_0 \Delta V = e_0 (_\alpha \Delta_{\alpha'} \psi) = W_e^\alpha - W_e^{\alpha'} \qquad (15)$$

In other words, charge transfer happens between two metals of the same species under an external voltage ΔV. In fact, since no field can be sustained within the same species of a metal, this means the two surfaces of the same metal are electrified.

Comparing two scenarios shown in Figure 2, we can see both systems are under potential control without varying the number of electrons. This means the whole system is canonical while each of two metals in contact is GC. As shown in Section Potential control with half-cell and full-cell models, this can be realized through either counter-ion/pseudo-atom methods or finite-field methods.

Potential control with half-cell and full-cell models

Type I: GC-DFT and constant Fermi DFTMD

In GC-DFT, the number of electrons in the system is allowed to vary over time, which can be used to charge

an electrode. The electrode Fermi-level is then forced to become equal to $\widetilde{\mu}_e^{\text{target}}$. The change in Fermi level corresponds to a buildup in the double layer potential as shown in Equation (7). During constant Fermi-level DFTMD, the electrochemical potential is set to a target value during the self-consistent field (SCF) in practice. This calculation may be difficult to converge which is why multiple canonical DFT calculations were often used instead to approximate the GC ensemble [17]. Another approach by Bonnet et al. to achieve this is to devise a potentiostat scheme where the calculation of the number of electrons is separated from the optimization of the electronic states [18]. The potential energy of the system in contact with an electron reservoir at $\widetilde{\mu}_e^{\text{target}}$ is

$$E_{\text{tot}} = E(R, n_e) + \widetilde{\mu}_e^{\text{target}} n_e \qquad (16)$$

and the derivative with respect to the number of electrons can be interpreted as a fictitious force:

$$F_{n_e} = -\frac{\partial E_{\text{tot}}}{\partial n_e} = \widetilde{\mu}_e^{\text{M}} - \widetilde{\mu}_e^{\text{target}} \qquad (17)$$

Now, we can let the electronic charge be a dynamical variable governed by

$$\dot{n}_e = \frac{p_{n_e}}{m_{n_e}}, \quad \dot{P}_{n_e} = F_{n_e} = \widetilde{\mu}_e^{\text{M}} - \widetilde{\mu}_e^{\text{target}} \qquad (18)$$

where p_{n_e} and m_{n_e} are fictitious momentum and mass. The fluctuation of the number of electrons about $\langle n_e \rangle$ then allows for sampling the GC ensemble to make $\langle \widetilde{\mu}_e^{\text{M}} \rangle = \widetilde{\mu}_e^{\text{target}}$.

This method was used by Bouzid and Pasquarello [19] to study the charged Pt(111)-water interface. With the addition of a hydronium ion to the system, the electrode potential can be aligned to the standard hydrogen electrode (SHE) by considering hydrogen adsorbed to Pt as an intermediate step in the SHE reaction, similar to the proton insertion method that developed for doing the band alignment at the semiconductor−water interfaces [20]. This allowed them to relate properties of the interface, such as double layer capacitance, to experiment.

The setup for constant Fermi-level DFTMD is a half cell. The electrode charge then has to be compensated somehow to make the overall system charge neutral under PBCs. Bonnet et al. used an electronic screening medium whereas Bouzid and Pasquarello made use of a homogeneous background charge. The homogenous background charge results in spurious interactions and corrections to the energy and potential have to be included [21]. Therefore, the key difference between different methods in the Type I category is about how

the electrolyte model (therefore, counter-charge) is designed and implemented. Indeed, various implicit solvation models have been developed for this purpose [22−25].

It is worth noting that simulations of the metal-electrolyte interface with GC-DFT can be done without explicitly referencing the Fermi-level. This point was illustrated by the constant inner potential (CIP) DFT method from Melander et al. [26]. If the inner potential in bulk solution is set to zero for both neutral and charged interfaces, $\phi_S = 0$, then following Equation (6) the double layer potential is

$$\phi_{EDL} = \phi^M - \phi^M_{\sigma=0}. \tag{19}$$

ϕ^M can be controlled by setting a constraint on the average potential in the bulk electrode.

Type II: counter-ion/pseudo-atom methods
In a full cell setup with two electrodes of the same metal, constant Fermi-level DFT cannot be used to induce a potential bias since the system only has one Fermi level. From the example in Figure 3a, however, a system with two different metals in contact will have a potential bias across the cell stemming from the charge transfer induced by the equalization of their Fermi levels. A similar situation can also happen when a metal is put into contact with a charged semiconductor/insulator. If the Fermi level of the metal is in the band gap of the charged semiconductor/insulator, then any excess charge is going to transfer to the metal.

Surendralal et al. [27] exploited this idea to control the potential of the anodic Mg/water interface using doped (pseudoatom) Ne as a counter-electrode. Ne was chosen for its large band gap and its valence band maximum/conduction band minimum relative to water. To generate a surplus or shortage of electrons in the system, the number of valence electrons and proton charge of each of the n_{Ne} Ne atoms is changed by a fraction q/n_{Ne}. This way, the total system stays charge neutral while each electrode obtains a charge q. To maintain a constant potential in the cell, the counter-electrode charge can be altered during the dynamics. Similarly, in the work by Le et al. [28], the Pt electrode is charged by adding Na/F atoms close to its surface. Khatib et al. [29] used the same strategy in their ion imbalance method but with Na/Cl atoms instead. In these setups, the electrode charge is constant (corresponding to the ion charge) while the double layer potential ϕ_{EDL} fluctuates. Although the double-layer can be modeled effectively in this manner, it is worth noting that the ion distribution is not fully in equilibrium.

Type III: finite-field methods
Recently, Dufils et al. [30] showed that constant potential simulation with the Siepmann-Sprik (SS) model which is commonly used together with 2D PBCs can be also realized with 3D PBCs and the finite-field methods [31].

The basis of the SS model [32,33] is to allow the electrode charges to fluctuate in response to the external potential, which mimics the physical process of an ideal polarizable electrode. Although the original model was built for simulating metal−water interfaces under potential bias, its applications to electrochemical interfaces with electrolyte solution are straightforward.

In the SS model, each response charge of the electrode atoms follows a Gaussian distribution of magnitude c_i centered on the position of the electrode atom $\mathbf{R}_i$

$$\rho_i(\mathbf{r}) = c_i \left(\frac{\zeta_i}{\pi}\right)^{3/2} \exp^{-\zeta_i(\mathbf{r}-\mathbf{R}_i)^2} \tag{20}$$

where ζ_i is an adjustable parameter related to the Gaussian width.

The original model at zero applied potential can be rewritten as follows using the chemical potential equalization ansatz [34].

$$U = U_0 + U_{q_0-\Delta\nu} + \frac{1}{2}\mathbf{c}^\top \boldsymbol{\eta}\mathbf{c} + \Delta\boldsymbol{\nu}^\top \mathbf{c} \tag{21}$$

where U_0 corresponds to the energy of electrode atoms in the absence of an external potential (field). The term $U_{q_0-\Delta\nu}$ corresponds to the electrode-electrolyte interaction (so electrostatic interactions between the atomic charges of electrolyte atoms and the base charges $\mathbf{q}_0$ of electrode atoms plus their van der Waals interactions). $\boldsymbol{\eta}$ is the hardness kernel, describing the interaction between response charges, and $\Delta\boldsymbol{\nu}$ is the potential generated by the electrolyte at the electrode atom sites. This energy is minimized with respect to the response charge $\mathbf{c}$ at each MD time-step under the constraint of charge neutrality.

With this model, a full-cell setup can be realized with two electrodes kept at constant potentials. If one electrode is set at zero potential, we can enforce a constant potential difference $\Delta\psi$ between the electrodes by altering the model Hamiltonian as

$$U_{\Delta\psi} = U - \sum_j \Delta\psi c_j, \tag{22}$$

where the sum is over all charges belonging to one electrode. This requires an electrolyte centered cell and the use of 2D PBCs, which makes the potential calculation computationally more expensive than the Ewald summation with 3D PBCs.

Figure 3
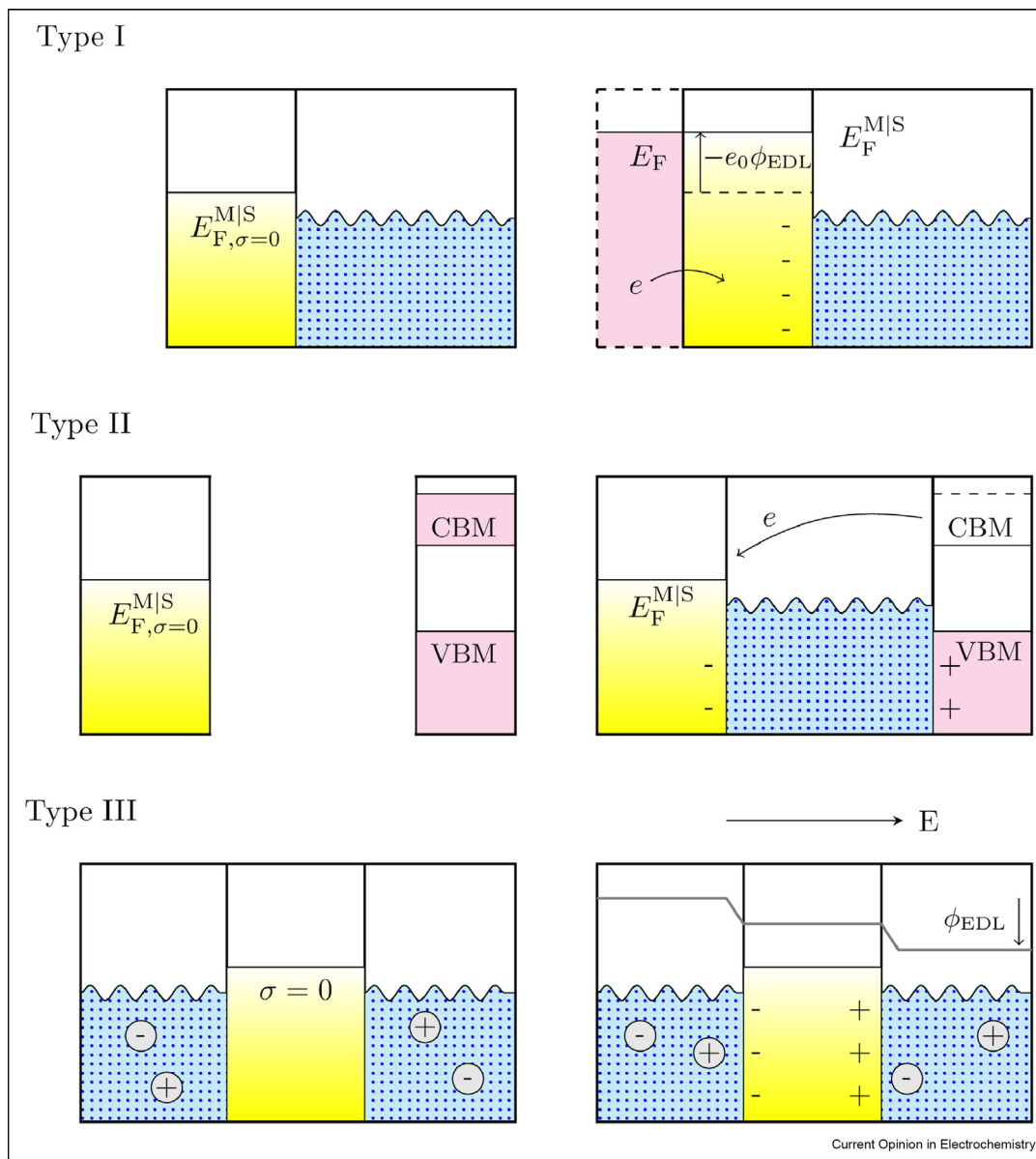
Three types of methods to impose the potential control for molecular dynamics simulations of metal-electrolyte interfaces. Type I: Grand canonical methods; Type II: Counter-ion/pseudo-atom methods; Type III: Finite-field methods. The dashed region is not part of the simulation box.

Instead, with the finite-field methods and 3D PBCs, the electrode charges are now coupled to an applied electric field E through

$$U_E = U - \Omega E P_z \tag{23}$$

where $P_z = \frac{1}{\Omega}\mathbf{R}_z \cdot (\mathbf{c} + \mathbf{q_0})$ is the polarization in the direction of the electric field. In this scenario, one electrode with a single inner potential was employed instead and we can use an electrode centered cell. The cell potential bias now comes from the different charges at the two electrode surfaces, in analogy with the example in Figure 2b. Knowing the constant E field directly leads to constant potential

simulation under 3D PBCs, applying a potentiostat on top of constant D simulations [35,36] may seem to be a detour. Nevertheless, interesting attempts have been made to control the potential difference using the constant electric displacement D Hamiltonian, which generates a constant $\langle E \rangle$ ensemble instead [37].

Potential of metal versus potential of electrolyte

So far, the focus of our discussions is on the potential control of metal. However, in an electrochemical cell with an active redox couple, electrons can transfer between electrodes and solution. If we attempt to control

the potential by just fixing the electrochemical potential of the metal electrode, $\widetilde{\mu}_e^{\mathrm{M}}$, there is no guarantee that the electrode potential is in equilibrium with the redox couple within the time scale of simulation. For the chemical reaction

$$\mathrm{O} + ne \rightleftharpoons \mathrm{R} \tag{24}$$

it is in equilibrium only if

$$\widetilde{\mu}_e^{\mathrm{M}} = \widetilde{\mu}_{\mathrm{R}}^{\mathrm{s}} - \widetilde{\mu}_{\mathrm{O}}^{\mathrm{s}}, \tag{25}$$

Otherwise, the system is under an overpotential. This means the electrified interface requires the counter-ions to form a concentration gradient in equilibrium. Therefore, to simulate an electrochemical cell under constant potential conditions, it is crucial to also take into account the potential of the electrolyte.

This is indeed very challenging as it requires a GC ensemble for the ions and the corresponding equilibration times goes far beyond the reach of standard AIMD simulations. As a matter of fact, a number of selected works listed in Table 1 only used water instead of electrolyte solution when building a solid-liquid interfacial system. Therefore, strictly speaking, these setups simulated a (nano)capacitor rather than an electrochemical interface.

Despite being challenging, potential control of the electrolyte can be achieved in various ways. With the help of liquid state theories, a molecular description of the electrolyte can be introduced, e.g. in joint DFT [38,39] where the solution is described by classical DFT [40] or in conjunction with the reference interaction site method [41,42]. With these descriptions of the electrolyte, the effect of an ion reservoir can be achieved, comparable to the electron reservoir in Type I methods. In Type II and III methods, explicit ions and electrolyte solution can be introduced and one can explore the classical MD simulation to speed-up the

equilibration of the electrolyte solution and bring counter-ions to their equilibrium positions next to the electrified interfaces. Similar to the case of metal in Type II and III methods where two sides of electrode are under GC condition but the whole piece of metal is still canonical, the same principle also applies to the electrolyte solution for its potential control.

Summary and outlook
In this short review, we have sorted the computational methods for potential control in MD simulations of the metal-electrolyte interface into three categories. In general, the potential control can be achieved either through a GC treatment of a half-cell model or a canonical treatment of the full-cell model. In both cases, charge transfer is induced by equalization of the Fermi level of a system by the exchange of electrons with an external reservoir or via redistribution of electrons within the system.

Work is still in progress on applying the finite-field methods to DFTMD simulations of the metal-electrolyte interface. In particular, it is interesting to see how the constant electric displacement method, that has been shown to be useful to compute Helmholtz capacitance of protonic double layers at metal oxide-electrolyte interface [43,44], can be also applied to the metal-electrolyte interfaces.

Finally, it is impossible not to mention machine-learning potentials (MLP) when discussing MD simulations nowadays. Indeed, a number of implementations toward the goal of modeling electrochemical systems using machine-learning accelerated atomistic simulations have emerged [45,46]. Their further developments and the full harnessing of the scalability of MLPs are expected to play a crucial role in the future of DFTMD simulations of electrified interfaces beyond slab geometry and short dynamics.

Declaration of competing interest
The authors declare that they have no known competing financial interests or personal relationships that could have appeared to influence the work reported in this paper.

Data availability
No data was used for the research described in the article.

Table 1

Examples of molecular dynamics simulations of metal-electrolyte systems under potential control.

Ref.	Type	Cell	Electrolyte	Charge neutrality	SHE	PBC
[18]	I	Half	None	ESM	No	2D
[19]	I	Half	Water + H_3O^+	Background charge	Yes	3D
[27]	II	Full	Water	Pseudo-atom	No	3D
[28]	II	Half	Water + ions	Counter-ion	Yes	3D
[30]	III	Full	Water + ions	Constraint	No	3D

References

Papers of particular interest, published within the period of review, have been highlighted as:

* of special interest
* * of outstanding interest

1. Schmickler W, Santos E: *Interfacial electrochemistry*. Berlin; London: Springer; 2010.

2. Mermin ND: **Thermal properties of the inhomogeneous electron gas**. *Phys Rev* 1965, **137**:A1441−A1443.

3. Lozovoi AY, Alavi A, Kohanoff J, Lynden-Bell RM: **Ab initio simulation of charged slabs at constant chemical potential**. *J Chem Phys* 2001, **115**:1661−1669.

4. Skúlason E, Karlberg GS, Rossmeisl J, Bligaard T, Greeley J, Jónsson H, Nørskov JK: **Density functional theory calculations for the hydrogen evolution reaction in an electrochemical double layer on the Pt(111) electrode**. *Phys Chem Chem Phys* 2007, **9**:3241−3250.

5. Rossmeisl J, Skúlason E, Björketun ME, Tripkovic V, Nørskov JK: **Modeling the electrified solid−liquid interface**. *Chem Phys Lett* 2008, **466**:68−71.

6. Price DL, Halley JW: **Molecular dynamics, density functional theory of the metal−electrolyte interface**. *J Chem Phys* 1995, **102**:6603−6611.

7. Groß A, Sakong S: **Modelling the electric double layer at electrode/electrolyte interfaces**. *Curr Opin Electrochem* 2019, **14**:1−6.

8. Huang J, Eikerling M: **Modeling the oxygen reduction reaction at platinum-based catalysts: a brief review of recent developments**. *Curr Opin Electrochem* 2019, **13**:157−165.

9. Le J-B, Yang X-H, Zhuang Y-B, Jia M, Cheng J: **Recent progress toward ab initio modeling of electrocatalysis**. *J Phys Chem Lett* 2021, **12**:8924−8931.

10. Scalfi L, Salanne M, Rotenberg B: **Molecular simulation of electrode-solution interfaces**. *Annu Rev Phys Chem* 2021, **72**:189−212.

11. Abidi N, Lim KRG, Seh ZW, Steinmann SN: **Atomistic modeling of electrocatalysis: are we there yet?** *WIRES Comput. Mol. Sci* 2021, **11**:e1499.

12. Sundararaman R, Vigil-Fowler D, Schwarz K: **Improving the accuracy of atomistic simulations of the electrochemical interface**. *Chem Rev* 2022, **122**:10651−10674.

13. Morgan LM, Mercer MP, Bhandari A, Peng C, Islam MM, Yang H, Holland Ji, Coles SW, Sharpe R, Walsh A, Morgan BJ, Kramer D, Islam MS, Hoster HE, Edge JS, Skylaris C-K: **Pushing the boundaries of lithium battery research with atomistic modelling on different scales**. *Prog. Energy* 2022, **4**, 012002.

14. Pedroza LS, Brandimarte P, Rocha AR, Fernández-Serra M-V: **Bias-dependent local structure of water molecules at a metallic interface**. *Chem Sci* 2017, **9**:62−69.

15. Cheng J, Sprik M: **Alignment of electronic energy levels at electrochemical interfaces**. *Phys Chem Chem Phys* 2012, **14**, 11245.

16. Trasatti S: **The work function in electrochemistry**. In *Advances in electrochemistry and electrochemical engineering: v.10*. Edited by Gerischer H, Tobias CW, Nashville, TN: John Wiley & Sons; 1977:213−321.

17. Kastlunger G, Lindgren P, Peterson AA: **Controlled-potential simulation of elementary electrochemical reactions: proton discharge on metal surfaces**. *J Phys Chem C* 2018, **122**:12771−12781.

18. Bonnet N, Morishita T, Sugino O, Otani M: **First-Principles molecular dynamics at a constant electrode potential**. *Phys Rev Lett* 2012, **109**:266101−266105.

19. Bouzid A, Pasquarello A: **Atomic-scale simulation of electrochemical processes at electrode/water interfaces under referenced bias potential**. *J Phys Chem Lett* 2018, **9**: 1880−1884.

20. Cheng J, Sprik M: **Aligning electronic energy levels at the TiO$_2$/H$_2$O interface**. *Phys Rev B* 2010, **82**, 081406.

21. Filhol J-S, Neurock M: **Elucidation of the electrochemical activation of water over pd by first principles**. *Angew Chem Int Ed* 2006, **45**:402−406.

22. Sundararaman R, Goddard WA: **The charge-asymmetric nonlocally determined local-electric (CANDLE) solvation model**. *J Chem Phys* 2015, **142**, 064107.

23. Ringe S, Oberhofer H, Reuter K: **Transferable ionic parameters for first-principles Poisson-Boltzmann solvation calculations: neutral solutes in aqueous mo novalent salt solutions**. *J Chem Phys* 2017, **146**, 134103.

24. Hörmann NG, Andreussi O, Marzari N: **Grand canonical simulations of electrochemical interfaces in implicit solvation models**. *J Chem Phys* 2019, **150**, 041730.

25. Bhandari A, Peng C, Dziedzic J, Anton L, Owen JR, Kramer D, Skylaris C-K: **Electrochemistry from first-principles in the grand canonical ensemble**. *J Chem Phys* 2021, **155**, 024114.

26. Melander M, Wu T, Honkala K: **Constant inner potential DFT for modelling electrochemical systems under constant potential and bias**. *chemrxiv-2021-r621x-v3* 2023:1−38.
* * Constant inner potential instead of constant Fermi level was introduced for the potential control.

27. Surendralal S, Todorova M, Finnis MW, Neugebauer J: **First-Principles approach to model electrochemical reactions: understanding the fundamental mechanisms behind Mg corrosion**. *Phys Rev Lett* 2018, **120**, 246801.

28. Le J-B, Fan Q-Y, Li J-Q, Cheng J: **Molecular origin of negative component of Helmholtz capacitance at electrified Pt(111)/water interface**. *Sci Adv* 2020, **6**, eabb1219.
* * The ion imbalance method used in DFTMD simulations was first introduced.

29. Khatib R, Kumar A, Sanvito S, Sulpizi M, Cucinotta CS: **The nanoscale structure of the Pt-water double layer under bias revealed**. *Electrochim Acta* 2021, **391**, 138875.
* The name of ion imbalance method was coined in this work.

30. Dufils T, Jeanmairet G, Rotenberg B, Sprik M, Salanne M: **Simulating electrochemical systems by combining the finite field method with a constant potential electrode**. *Phys Rev Lett* 2019, **123**, 195501.
* * A proof-of-concept study using the finite-field molecular dynamics simulations for potential control with the Siepmann-Sprik-type model.

31. Zhang C, Sayer T, Hutter J, Sprik M: **Modelling electrochemical systems with finite field molecular dynamics**. *JPhys Energy* 2020, **2**, 032005.

32. Siepmann JI, Sprik M: **Influence of surface topology and electrostatic potential on water/electrode systems**. *J Chem Phys* 1995, **102**:511−524.

33. Reed SK, Lanning OJ, Madden PA: **Electrochemical interface between an ionic liquid and a model metallic electrode**. *J Chem Phys* 2007, **126**, 084704.

34. York DM, Yang W: **A chemical potential equalization method for molecular simulations**. *J Chem Phys* 1996, **104**:159−172.

35. Stengel M, Spaldin NA, Vanderbilt D: **Electric displacement as the fundamental variable in electronic-structure calculations**. *Nat Phys* 2009, **5**:304−308.

36. Zhang C, Sprik M: **Computing the dielectric constant of liquid water at constant dielectric displacement**. *Phys Rev B* 2016, **93**, 144201.

37. Deißenbeck F, Freysoldt C, Todorova M, Neugebauer J, Wippermann S: **Dielectric properties of nanoconfined water: a canonical thermopotentiostat approach**. *Phys Rev Lett* 2021, **126**, 136803.
* An alternative formulation of the finite-field methods for implementing potentiostat.

38. Petrosyan SA, Briere J-F, Roundy D, Arias TA: **Joint density-functional theory for electronic structure of solvated systems**. *Phys Rev B* 2007, **75**, 205105.

39. Letchworth-Weaver K, Arias TA: **Joint density functional theory of the electrode-electrolyte interface: application to fixed electrode potentials, interfacial capacitances, and potentials of zero charge**. *Phys Rev B* 2012, **86**, 075140. 16.

40. Wu J: **Understanding the electric double-layer structure, capacitance, and charging dynamics**. *Chem Rev* 2022, **122**: 10821−10859.

41. Chandler D, Andersen HC: **Optimized cluster expansions for classical fluids. II. Theory of molecular liquids**. *J Chem Phys* 1972, **57**:1930−1937.

42. Nishihara S, Otani M: **Hybrid solvation models for bulk, interface, and membrane: reference interaction site methods coupled with density functional theory**. *Phys Rev B* 2017, **96**, 115429.

43. Zhang C, Hutter J, Sprik M: **Coupling of surface chemistry and electric double layer at TiO$_2$ electrochemical interfaces**. *J Phys Chem Lett* 2019, **10**:3871−3876.

44. Jia M, Zhang C, Cheng J: **Origin of asymmetric electric double layers at electrified oxide/electrolyte interfaces**. *J Phys Chem Lett* 2021, **12**:4616−4622.

45. Dufils T, Knijff L, Shao Y, Zhang C: **PiNNwall: heterogeneous**
** **electrode models from integrating machine learning and atomistic simulation**. *J Chem Theor Comput* 2023, **19**: 5199−5209.
The first of its kind for integrating atomistic machine learning into the finite-field molecular dynamics simulations of electrochemical interfaces.

46. Grisafi A, Bussy A, Vuilleumier R: **Predicting the charge density response in metal electrodes**. *arXiv:2304.08966v2* 2023: 1−6.